THE JOURNAL OF BIOLOGICAL CHEMISTRY VOL. 291, NO. 45, pp. 23452–23463, November 4, 2016

Unorthodox Acetylcholine Binding Sites Formed by α5 and β3 Accessory Subunits in α4β2* Nicotinic Acetylcholine Receptors*

Received for publication, July 19, 2016, and in revised form, September 6, 2016 Published, JBC Papers in Press, September 19, 2016, DOI 10.1074/jbc.M116.749150

Akansha Jain[‡], Alexander Kuryatov[‡], Jingyi Wang[§], Theodore M. Kamenecka[¶], and Jon Lindstrom[‡1]

From the [‡]Department of Neuroscience, Perelman School of Medicine at the University of Pennsylvania, Philadelphia, Pennsylvania 19104, the [§]Division of Pharmacology and Toxicology, College of Pharmacy, The University of Texas at Austin, Austin, Texas 78712, and the [¶]Department of Molecular Therapeutics, Scripps Research Institute, Jupiter, Florida 33458

All nicotinic acetylcholine receptors (nAChRs) evolved from homomeric nAChRs in which all five subunits are involved in forming acetylcholine (ACh) binding sites at their interfaces. Heteromeric α4β2* nAChRs typically have two ACh binding sites at α4/β2 interfaces and a fifth accessory subunit surrounding the central cation channel. β2 accessory subunits do not form ACh binding sites, but α4 accessory subunits do at the α4/α4 interface in $(\alpha4\beta2)_2\alpha4$ nAChRs. α5 and β3 are closely related subunits that had been thought to act only as accessory subunits and not take part in forming ACh binding sites. The effect of agonists at various subunit interfaces was determined by blocking homologous sites at these interfaces using the thioreactive agent 2-((trimethylammonium)ethyl) methanethiosulfonate (MTSET). We found that α5/α4 and β3/α4 interfaces formed ACh binding sites in $(\alpha4\beta2)_2\alpha5$ and $(\alpha4\beta2)_2\beta3$ nAChRs. The α4/α5 interface in $(\beta2\alpha4)_2\alpha5$ nAChRs also formed an ACh binding site. Blocking of these sites with MTSET reduced the maximal ACh evoked responses of these nAChRs by 30–50%. However, site-selective agonists NS9283 (for the α4/α4 site) and sazetidine-A (for the α4/β2 site) did not act on the ACh sites formed by the α5/α4 or β3/α4 interfaces. This suggests that unorthodox sites formed by α5 and β3 subunits have unique ligand selectivity. Agonists or antagonists for these unorthodox sites might be selective and effective drugs for modulating nAChR function to treat nicotine addiction and other disorders.

Nicotinic acetylcholine receptors (nAChRs)[2] are ACh-gated ion channels formed from five homologous subunits organized like barrel staves around a central cation channel (1). There are homomeric nAChRs and heteromeric nAChRs. Homomeric α7 nAChRs have five α7 subunits with ACh binding sites between each of the five α7/α7 interfaces. All nAChR subunits exhibit basic homology throughout their sequences, indicating that all nAChRs evolved from a common ancestor (1, 2). Heteromeric nAChR agonist binding sites typically form at the interface between the primary (+) side of an α subunit, characterized by the presence of a C loop that closes over the site when the nAChR is activated by an agonist, and the complementary (−) side of a β2 or β4 subunit (3). Two such ACh binding sites assemble with an accessory subunit in a stoichiometry such as $(\alpha4\beta2)_2\beta2$ (4, 5).

The $(\alpha4\beta2)_2\alpha4$ stoichiometry contains an unorthodox ACh binding site at the α4/α4 interface (6, 7). When this low affinity unorthodox site is bound by ACh or NS9283, an agonist specific for this site, nAChRs activate 3–4-fold more efficiently (8, 9). Blocking the α4/α4 site through alkylation of a cysteine introduced in the minus face of the α4 subunit blocked the activity of ACh and NS9283 (9). Histidine 142 (this is position 116 in the mature α4 peptide sequence) on the minus side of α4 is critical for the binding of NS9283 (10). Sazetidine-A is a high affinity agonist selective for α4/β2 sites that cannot bind to the α4/α4 interface because histidine 142 on the minus side of α4 prevents it from binding, whereas this amino acid is valine in β2 (11, 12). Because orthodox agonist sites are shared among nAChRs, subtype selectivity is more likely to be achieved by targeting unorthodox agonist sites.

It has been assumed that α5 and β3 function only as accessory subunits, and it is unknown whether they contribute to forming agonist binding sites (13–15). These subunits are closely related in sequence, but α5 has a cysteine pair at the tip of its C loop that defines it as an α subunit, and β3 does not. $(\alpha4\beta2)_2\alpha5$ and $(\alpha4\beta2)_2\beta3$ nAChRs are found in the brain, as are $(\alpha6\beta2)(\alpha4\beta2)\beta3$ nAChRs (3, 16–20). α5 and β3 subunits have been implicated in nicotine addiction and are likely to be involved in many diseases associated with nAChRs (21–26). An α5 D398N and some β3 polymorphisms are associated with susceptibility to smoking (26, 27). The α5 polymorphism is also associated with susceptibility to lung cancer (26). Knock-out of α4, α6, or β2 subunits inhibits the rewarding properties and self-administration of nicotine (28), whereas knock-out of α5 inhibits the aversive effects of high nicotine concentrations and increases self-administration of nicotine (29). Thus, a drug that increases the function of α5* nAChRs might increase aversion to nicotine and promote cessation of smoking.

Unorthodox ACh binding sites are likely to be especially specific drug targets because α4/α4, α5/α4, and β3/α4 ACh bind-

* This work was supported in part by National Institutes of Health National Institute on Drug Abuse Grant DA030929. The authors declare that they have no conflicts of interest with the contents of this article. The content is solely the responsibility of the authors and does not necessarily represent the official views of the National Institutes of Health.

[1] To whom correspondence should be addressed: Dept. of Neuroscience, Perelman School of Medicine of the University of Pennsylvania, 130A John Morgan Bldg., Philadelphia, PA 19104-6074. Tel.: 215-573-2859; Fax: 215-573-2858; E-mail: JSLKK@mail.med.upenn.edu.

[2] The abbreviations used are: nAChR, nicotinic acetylcholine receptor; ACh, acetylcholine; NS9283, 3-[3-(pyridyl)-1,2,4-oxadiazol-5-yl]benzonitrile; MTSET, 2-(trimethylammonium)ethyl)methanethiosulfonate.

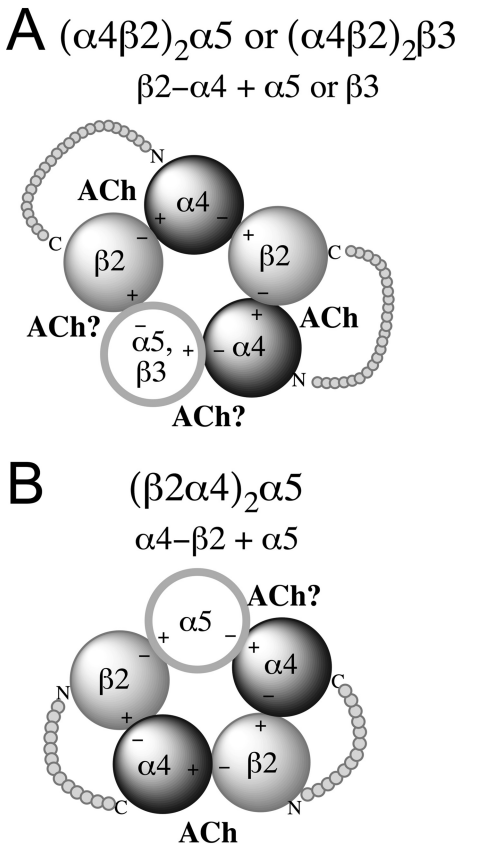

FIGURE 1. **Schematic diagram of $(\alpha4\beta2)_2\alpha5$, $(\alpha4\beta2)_2\beta3$, and $(\beta2\alpha4)_2\alpha5$ nAChRs.** *A*, this illustrates how the $\beta2$-$\alpha4$ dimeric concatamer plus the free $\alpha5$ or $\beta3$ subunit is thought to assemble into nAChRs. *B*, this illustrates how the $\alpha4$-$\beta2$ dimeric concatamer plus the free $\alpha5$ or $\beta3$ subunit is thought to assemble into nAChRs. Functional agonist sites, + and − sides of subunits, and $(AGS)_6$ linkers between the C terminus to the N terminus are illustrated. Existence of ACh sites at $\alpha5/\alpha4$, $\beta2/\alpha5$, $\beta3/\alpha4$, $\beta2/\beta3$, and $\alpha4/\alpha5$ will be explored in subsequent experiments.

ing sites have unique structural features compared with orthodox sites formed from combinations of $\alpha2$, $\alpha3$, $\alpha4$, or $\alpha6$ subunits with $\beta2$ or $\beta4$ or $\alpha7/\alpha7$ sites. Unorthodox sites are formed by incorporating $\alpha4$ or $\alpha5$ and perhaps other α and $\beta3$ subunits in pairs that do not include $\beta2$ or $\beta4$ subunits.

In this study, the effect of agonists at various subunit interfaces was determined through the selective blockage of specific subunit interfaces with the thioreactive agent, MTSET. Here we show that unorthodox ACh binding sites can form at the $\alpha5/\alpha4$ and $\beta3/\alpha4$ interfaces in $(\alpha4\beta2)_2\alpha5$ and $(\alpha4\beta2)_2\beta3$ nAChRs and at the $\alpha4/\alpha5$ in $(\beta2\alpha4)_2\alpha5$ nAChRs.

Results

Model Depicting nAChRs Formed by Concatamers—To study ACh homologue sites formed by $\alpha4$ with $\alpha5$ or $\beta3$ subunits, we constructed these subunit interfaces using concatamers with $\alpha4$ and $\beta2$ subunits linked in different orders (Fig. 1). These illustrations are important for understanding the different concatamers used to form desired interfaces, such as the $\alpha5/\alpha4$ interface *versus* the $\alpha4/\alpha5$ interface. To represent the assembled orientation of linked subunits, nAChRs assembled from $\beta2$-$\alpha4$ and a free subunit are noted as $(\alpha4\beta2)_2$*. Correspondingly, $(\beta2\alpha4)_2$* represents nAChRs assembled from a $\alpha4$-$\beta2$ concatamer.

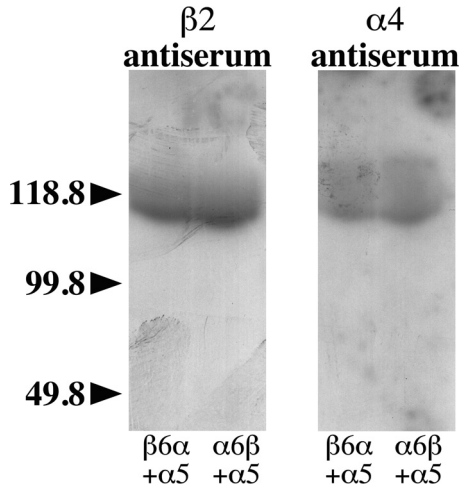

FIGURE 2. **Western blots of wild type β-6-α and α-6-β concatamers co-expressed with $\alpha5$ in oocytes.** Expression of the concatamers β-6-α and α-6-β was detected by rat antisera to $\beta2$ or $\alpha4$ followed by ^{125}I-labeled goat anti-rat IgG (2 nM). After washing, the blots were visualized by autoradiography. The Western blots showed that concatamers were not degraded to form any free subunits and that β-6-α and α-6-β migrated at a molecular mass of ~118 kDa. On each lane the equivalent of half of an oocyte was loaded. These data also demonstrated that the concatamer cRNAs were properly translated in the oocytes, and no degradation to unlinked subunits (~70 kDa for $\alpha4$ and ~57 kDa for $\beta2$) was seen.

Fig. 1*A* illustrates how $\beta2$-$\alpha4$ dimeric concatamer plus free $\alpha5$ or $\beta3$ subunit is thought to assemble into nAChRs. Concatamers are generated by connecting the C-tail of one subunit to the N terminus of the next. The order of the subunits around the cation channel can be determined by the length of the linker between the subunits (30). When the 23-amino acid-long C-terminal tail of $\beta2$ subunits is linked by $(AGS)_6$, or a longer linker to the N terminus of $\alpha4$, a binding site forms within the linked subunit pair to form an $\alpha4/\beta2$ ACh binding site (30). This allows the free subunit to assemble as an accessory subunit in combination with two $\alpha4/\beta2$ ACh binding sites.

Fig. 1*B* illustrates how $\alpha4$-$\beta2$ dimeric concatamer plus free $\alpha5$ subunit is thought to assemble into nAChRs. The linker of $\alpha4$-$\beta2$ dimeric concatamer is much shorter than that of the $\beta2$-$\alpha4$ dimeric concatamer. When the short 7-amino acid C-tail of $\alpha4$, compared with the 23-amino acid-long C-tail of $\beta2$, is linked by $(AGS)_6$ to the N terminus of $\beta2$, the subunits are constrained to assemble so that $\alpha4/\beta2$ ACh binding sites are formed between linked pairs of subunits, and $\alpha5$ assembles with the plus rather than minus face of $\alpha4$ to form an $\alpha4/\alpha5$ interface.

Immunoblots of Triton X-100 extracts from oocytes injected with concatamers confirmed the integrity of expressed proteins (Fig. 2). Concatamer β-6-α and α-6-β migrated at a molecular mass of ~118 kDa. These data demonstrated that concatamer cRNAs were properly translated in the oocytes, and no degradation to unlinked subunits was seen.

Pharmacological Properties of $(\alpha4\beta2)_2\alpha5$, $(\alpha4\beta2)_2\beta3$, and $(\beta2\alpha4)_2\alpha5$ nAChRs—Because the $\alpha4/\alpha4$ ACh site in $(\alpha4\beta2)_2\alpha4$ nAChRs changes the pharmacology of $\alpha4\beta2$ nAChRs (6, 12), $\alpha5$ and $\beta3$ subunits may alter agonist selectivity, potency, and efficacy of $\alpha4\beta2$ nAChRs if they form agonist sites with $\alpha4$. We used $\beta2$-$\alpha4$ or $\alpha4$-$\beta2$ concatamers with free subunits to express $(\alpha4\beta2)_2\alpha5$, $(\alpha4\beta2)_2\beta3$, and $(\beta2\alpha4)_2\alpha5$ nAChRs in *Xenopus*

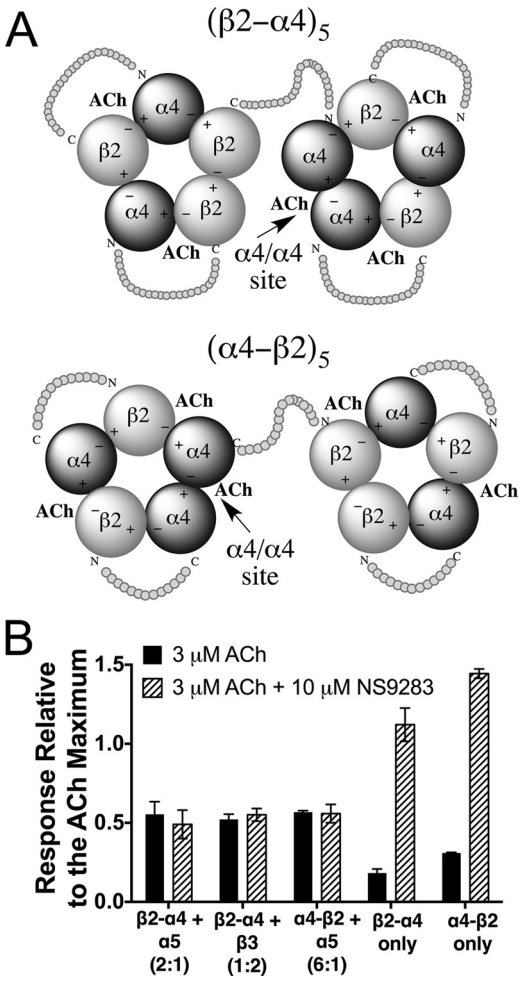

FIGURE 3. **Proof of assembly of free subunit with concatamers.** *A*, schematic illustration of dipentameric nAChRs thought to be formed by the β2-α4 and α4-β2 dimeric concatamers alone. The dipentamer is composed of five pairs of linked subunits forming two pentamers and joined by one pair of linked subunits. The α4/α4 site in the dipentameric nAChRs is illustrated. *B*, NS9283 increased activation of dipentameric nAChRs but not nAChRs expressed from concatamer and free subunit (β2-α4 and α4-β2 only *versus* β2-α4 + α5, β2-α4 + β3, and α4-β2 + α5). This suggests that sufficient β3 and α5 were used to ensure assembly of all concatamers into monopentamers.

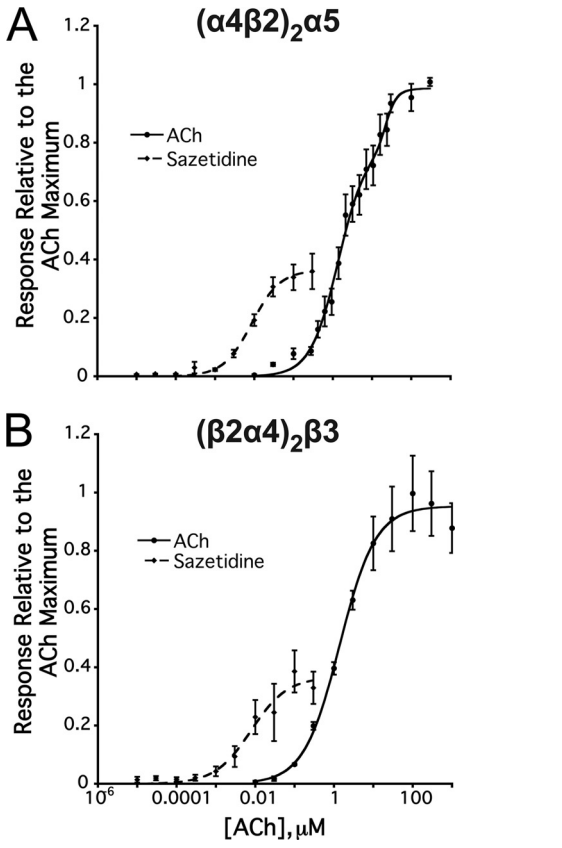

FIGURE 4. **ACh and Sazetidine-A concentration/response curves for $(\alpha4\beta2)_2\alpha5$ and $(\alpha4\beta2)_2\beta3$ nAChRs.** *A*, a biphasic ACh concentration/response curve was observed for $(\alpha4\beta2)_2\alpha5$ nAChRs. A high sensitivity EC_{50} = 1.38 ± 0.33 μM and a low sensitivity EC_{50} = 22.60 ± 5.75 μM were determined. Sazetidine-A is a partial agonist with I_{max} = 36.3 ± 1.01%. *B*, a biphasic ACh curve for $(\alpha4\beta2)_2\beta3$ nAChRs was not detected. A single high sensitivity EC_{50} = 1.56 ± 0.14 μM was determined. Sazetidine-A is a partial agonist with I_{max} = 33.2 ± 4.9%. I_{max} is the maximum current peak at the saturating concentration.

oocytes. We first evaluated whether α5 and β3 subunits efficiently incorporated with dimeric concatamers.

If α5 or β3 failed to assemble with dimeric concatamers, the functional responses should represent activation of dimeric pentamers resulting from self-assembly of β2-α4 and α4-β2 (Fig. 3*A*) (30). These dimeric pentamers contain an α4/α4 interface (Fig. 3*A*). We used NS9283 to test for the presence of dimeric pentamers because this compound acts as a selective agonist for the α4/α4 ACh binding site (8, 9).

NS9283 increased the responses evoked by ACh almost 6-fold when dimeric concatamers alone were expressed in *Xenopus* oocytes (Fig. 3*B*). However, when the dimeric concatamers were expressed with free α5 or β3, NS9283 did not potentiate the responses (Fig. 3*B*). The absence of potentiation indicates that the cRNA ratios used to obtain $(\alpha4\beta2)_2\alpha5$, $(\alpha4\beta2)_2\beta3$, and $(\beta2\alpha4)_2\alpha5$ only formed monopentamers.

Then we characterized the activation of $(\alpha4\beta2)_2\alpha5$, $(\alpha4\beta2)_2\beta3$, and $(\beta2\alpha4)_2\alpha5$ nAChRs by ACh, nicotine, and various partial agonists. $(\alpha4\beta2)_2\alpha4$ nAChRs exhibited biphasic concentration/response curves with a high sensitivity component caused by the two α4/β2 sites (EC_{50} = ~0.7 μM ACh) and a 3–4-fold larger component caused by the third low sensitivity α4/α4 site (EC_{50} = ~80 μM ACh) (7, 12, 31, 32). Assaying $(\alpha4\beta2)_2\alpha5$ nAChRs using closely spaced ACh concentrations resolved a biphasic concentration/response curve (Fig. 4*A*). This suggests the presence of high sensitivity (EC_{50} = 1.38 ± 0.33 μM) ACh binding sites at the two α4/β2 interfaces and a lower sensitivity (EC_{50} = 22.6 ± 5.8 μM) ACh binding site at the α5/α4 interface (Table 1). $(\beta2\alpha4)_2\alpha5$ nAChRs exhibited a monophasic concentration/response curve with an EC_{50} of 1.25 ± 0.12 μM ACh.

A biphasic concentration/response curve was not resolved for $(\alpha4\beta2)_2\beta3$ nAChRs. A single EC_{50} (1.56 ± 0.14 μM) for ACh was determined (Fig. 4*B* and Table 1). This indicates that either β3/α4 sites have the same sensitivity as α4/β2 or the functional effect of β3/α4 sites is not detectable.

The potencies and efficacies of nicotine and various partial agonists were also determined (Table 1). Pharmacological profiles of the $(\alpha4\beta2)_2\alpha5$ and $(\alpha4\beta2)_2\beta3$ nAChRs were very similar. However, $(\alpha4\beta2)_2\alpha5$ nAChRs were 5-fold more sensitive to cytisine (EC_{50} = 0.501 ± 0.095 μM) than $(\alpha4\beta2)_2\beta3$ nAChRs

TABLE 1

Pharmacological profiles of $(\alpha4\beta2)_2\alpha5$, $(\alpha4\beta2)_2\beta3$, and $(\beta2\alpha4)_2\alpha5$ nAChRs for ACh, nicotine, and several partial agonists

The values for the EC_{50}, Hill coefficients, and their relative maximum efficacy to ACh are listed. ND represents values not determined. $n \geq 3$ for all concentration/response curves. HS and LS are the high sensitivity and low sensitivity components of the biphasic concentration/response curve, respectively.

	$(\alpha4\beta2)_2\alpha5$	$(\alpha4\beta2)_2\beta3$	$(\beta2\alpha4)_2\alpha5$
ACh			
Biphasic			
$EC_{50,HS}$ (μM)	1.38 ± 0.33	ND	ND
$EC_{50,LS}$ (μM)	22.6 ± 5.8		
Monophasic			
EC_{50} (μM)	1.85 ± 0.23	1.39 ± 0.33	1.24 ± 0.12
Efficacy (%)	99.0 ± 2.1	95.3 ± 2.1	94.4 ± 2.5
n_{Hill}	0.918 ± 0.074	0.951 ± 0.093	0.910 ± 0.049
Nicotine			
EC_{50} (μM)	0.951 ± 0.338	0.602 ± 0.110	0.487 ± 0.127
Efficacy (%)	35.4 ± 3.0	23.8 ± 1.2	59.1 ± 4.8
n_{Hill}	0.910 ± 0.154	1.32 ± 0.26	0.883 ± 0.060
Varenicline			
EC_{50} (μM)	0.139 ± 0.044	0.111 ± 0.043	0.058 ± 0.026
Efficacy (%)	11.5 ± 0.7	11.6 ± 0.8	14.4 ± 1.23
n_{Hill}	0.856 ± 0.189	0.560 ± 0.091	0.538 ± 0.045
Sazetidine-A			
EC_{50} (nM)	8.68 ± 0.92	7.08 ± 3.49	1.31 ± 0.30
Efficacy (%)	36.3 ± 1.0	33.2 ± 4.9	45.7 ± 2.6
n_{Hill}	1.20 ± 0.12	1.29 ± 0.45	1.17 ± 0.26
Cytisine			
EC_{50} (μM)	0.501 ± 0.085	2.52 ± 0.77	0.444 ± 0.090
Efficacy (%)	8.02 ± 0.44	11.0 ± 0.7	8.51 ± 0.34
n_{Hill}	0.973 ± 0.164	0.562 ± 0.057	0.852 ± 0.119

(EC_{50} = 2.25 ± 0.77 μM). Potencies and efficacies of nicotine, sazetidine-A, and varenicline were similar for both subtypes.

Sazetidine-A acts as a partial agonist for both $(\alpha4\beta2)_2\alpha5$ and $(\alpha4\beta2)_2\beta3$ nAChRs (Fig. 4) despite acting as a full agonist for the $(\alpha4\beta2)_2\beta2$ subtype (11). This is because sazetidine-A is only able to bind to two of the three sites, at the $\alpha4/\beta2$ interfaces, but not the third unorthodox site at the $\alpha5/\alpha4$ and $\beta3/\alpha4$ interfaces in which there is a histidine 142 at the minus face of $\alpha4$ to prevent binding of sazetidine-A (11, 12).

The pharmacological properties of $(\beta2\alpha4)_2\alpha5$ nAChRs were very similar to those of $(\alpha4\beta2)_2\alpha5$ nAChRs; however, $(\beta2\alpha4)_2\alpha5$ nAChRs were almost 3-fold more sensitive to varenicline and almost 2-fold more sensitive and efficacious to nicotine than $(\alpha4\beta2)_2\alpha5$ nAChRs (Table 1). In addition, nicotine was ~2-fold more efficacious for $(\alpha4\beta2)_2\alpha5$ nAChRs compared with $(\beta2\alpha4)_2\alpha5$ nAChRs. The difference in varenicline and nicotine sensitivities was within the range of error, but the difference in nicotine efficacies was not. Such pharmacological differences may result from the different assembly of the two subtypes. $(\alpha4\beta2)_2\alpha5$ nAChRs contain two $\alpha4/\beta2$ sites and one $\alpha5/\alpha4$ site, whereas $(\beta2\alpha4)_2\alpha5$ nAChRs contain only one $\alpha4/\beta2$ site and one $\alpha4/\alpha5$ site.

Cysteine Mutants Used to Study Specific Interfaces Formed by β3 and α5 Subunits—Because sazetidine-A is a partial agonist for $(\alpha4\beta2)_2\alpha5$, $(\alpha4\beta2)_2\beta3$, and $(\beta2\alpha4)_2\alpha5$ nAChRs, it is likely that sazetidine-A only binds to the $\alpha4/\beta2$ interfaces, but ACh binds to both the $\alpha4/\beta2$ and additional sites formed by $\beta3$ or $\alpha5$ subunits (Fig. 1). To test this hypothesis and evaluate which interfaces forms ACh sites, we mutated a cysteine at the minus site of various subunit interfaces (Figs. 5 and 6 and Table 2). Alkylation of this cysteine residue will block the ACh homologue sites in the corresponding subunit interfaces (9, 33). If this interface forms an agonist site, MTSET will block the activation of ACh. No change of response is expected if MTSET reacts with the cysteine at interfaces that do not bind an agonist (Figs. 5 and 6) (9, 33).

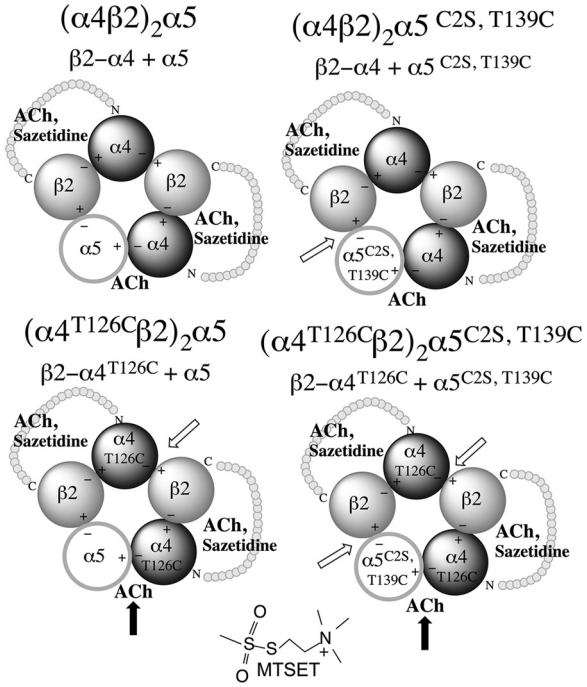

FIGURE 5. **Schematic illustration of alkylation of $(\alpha4\beta2)_2\alpha5$ nAChRs.** nAChRs were expressed from wild type or mutant $\beta2$-$\alpha4$ dimeric concatamers co-expressed with wild type or mutant $\alpha5$ subunits. The $\alpha4^{T126C}$ mutation was introduced to provide a cysteine at the minus face of the $\alpha5/\alpha4$ interface, and the $\alpha5^{T139C}$ mutation was introduced to provide a cysteine at the minus face of the $\beta2/\alpha5$ interface, where alkylation of the cysteine by MTSET allowed for the selective blockage of the desired interface. The free cysteine at position 2 of $\alpha5$ was mutated to a cysteine-null pseudo wild type $\alpha5^{C2S}$.

The $\alpha5/\alpha4$ and $\beta3/\alpha4$ interfaces can be selectively blocked by mutating threonine 126 on the minus face of the $\alpha4$ subunit to a cysteine residue followed by alkylation of the cysteine with MTSET. The $\beta2/\alpha5$ and $\beta2/\beta3$ sites were investigated by mutating the threonine 139 residue on the minus face of the $\alpha5$ subunit and mutating the threonine 123 residue on the minus face of the $\beta3$ subunit. The $\alpha5$ subunit contains a free cysteine at position 2. To prevent nonspecific modification or any potential disulfide formations between the single free cysteine at position 2, we mutated the cysteine to a serine (33). The mutations did not significantly change the level of expression. Maximum responses evoked by ACh were similar among WT and mutants: 1.62 ± 0.21 μA for $(\alpha4\beta2)_2\alpha5$, 1.78 ± 0.14 μA for $(\alpha4^{T126C}\beta2)_2\alpha5$, 1.21 ± 0.56 μA for $(\alpha4\beta2)_2\alpha5^{T139C}$, 1.11 ± 0.29 μA for $(\alpha4\beta2)_2\beta3$, 1.70 ± 0.37 μA for $(\alpha4^{T126C}\beta2)_2\beta3$, and 1.58 ± 0.45 μA for $(\alpha4\beta2)_2\beta2^{T123C}$ nAChRs.

The concentration of MTSET used for alkylation experiments was 0.5 mM for $\alpha5$ containing nAChRs because higher concentrations resulted in a significant decrease in the ACh response of wild type nAChRs. The concentration of MTSET used for alkylation experiments for $\beta3$ containing nAChRs was 2 mM, the concentration at which the wild type response was not affected after alkylation. With 5 mM MTSET, blockage (~30%) was similar to that with 2 mM.

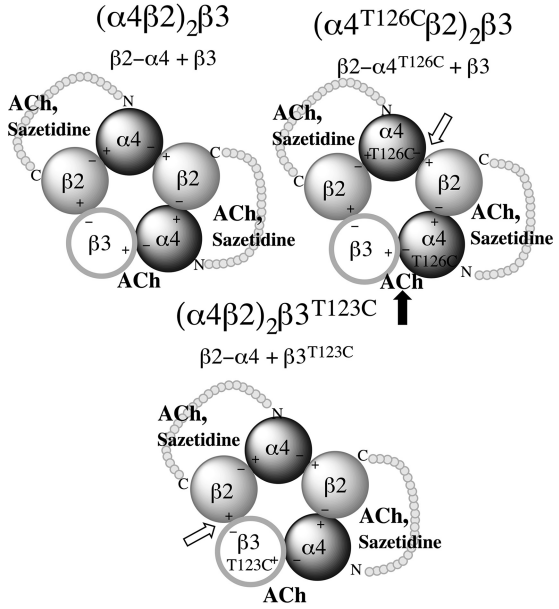

FIGURE 6. **Schematic illustration of alkylation of $(\alpha4\beta2)_2\beta3$ nAChRs.** nAChRs were expressed from wild type or mutant β2-α4 dimeric concatamers co-expressed with wild type or mutant β3 subunits. The $\alpha4^{T126C}$ mutation was introduced to provide a cysteine at the minus face of the β3/α4 interface, and the $\beta3^{T123C}$ mutation was introduced to provide a cysteine at the minus face of the β2/β3 interface, where alkylation of the cysteine allowed for the selective blockage of the desired interface by MTSET.

TABLE 2

Mutants used for MTSET alkylation experiments

Locations of mutations are underlined. Binding site mutations are in loop E on the minus side of the site. The C2S mutation is near the N terminus.

Mutant	Location of mutations
$\alpha4^{T126C}$	VQWTPPA
$\alpha5^{T139C}$	VTWTPPA
$\beta2^{L121C}$	IFWLPPA
$\beta3^{T123C}$	VVWTPPA
$\alpha5^{C2S}$	AGRCGLA

MTSET Blocks Activation from the α5/α4 Site—The β2-$\alpha4^{T126C}$ dimeric concatamer was expressed with α5 to allow blockage of the α5/α4 interface (Fig. 5). $(\alpha4^{T126C}\beta2)_2\alpha5$ nAChRs have intact agonist sites at the α4/β2 interfaces, a blockable site at the α5/α4 interface, and a blockable site at the nonfunctional β2/α4 interface (Fig. 5). Alkylation of the cysteine mutation at the β2/α4 interface does not block activation (9). Therefore, any decrease in response after MTSET treatment of $(\alpha4^{T126C}\beta2)_2\alpha5$ nAChRs can be attributed to specific block of the α5/α4 interface.

Wild type nAChRs were tested before and after MTSET treatment as a negative control for the mutant nAChRs (Fig. 7*A*). Incubation of oocytes with MTSET for 5 min reduced activation by ACh for $(\alpha4^{T126C}\beta2)_2\alpha5$ nAChRs by 45–50% of the original ACh response (Figs. 6*C* and 7*B*). Although response evoked by 30 μM ACh was blocked ~50% ($p = 0.0016$), MTSET did not significantly affect responses of wild type or mutant $(\alpha4\beta2)_2\alpha5$ nAChRs to a saturating (100 nM) concentration of sazetidine-A (Fig. 7*B*). This confirms the idea that sazetidine-A can bind to and activate α4/β2 sites but not α5/α4 sites, which have a histidine 142 residue on the minus side of α4 that prevents binding of sazetidine-A (10–12).

When $\alpha5^{C2S}$ was co-expressed with the β2-$\alpha4^{T126C}$ dimeric concatamer, there was no additional blockage by MTSET compared with using wild type α5, indicating that the block observed in the wild type α5 was solely due to blockage of activation by ACh at the α5/α4 interface (Fig. 7*D*).

Unlike the α5/α4 interface, the β2/α5 interface did not form a functional ACh binding site. When $\alpha5^{C2S,\ T139C}$ was co-expressed with the β2-α4 dimeric concatamer, the response after alkylation was similar to the wild type. In addition, when the β2-$\alpha4^{T126C}$ dimeric concatamer was co-expressed with $\alpha5^{C2S,\ T139C}$, there was no significant increase in the blockage as seen previously with $(\alpha4^{T126C}\beta2)_2\alpha5$ nAChRs (Fig. 7*E*).

This suggests that $(\alpha4\beta2)_2\alpha5$ nAChRs contain three functional ACh binding sites: two within the dimeric concatamers at the two α4/β2 interfaces and one at the α5/α4 interface. All the values for the ACh concentration/response curves before and after MTSET alkylation for α5 containing nAChRs are presented in Table 3.

MTSET Blocks Activation from the β3/α4 Site—β2-$\alpha4^{T126C}$ dimeric concatamer was expressed with the free β3 subunit to allow blockage of the β3/α4 interface (Fig. 6). Similarly to $(\alpha4^{T126C}\beta2)_2\alpha5$ nAChRs, these nAChRs have intact agonist sites at the α4/β2 interfaces, a blockable site at the accessory β3/α4 interface, and a blockable site at the nonfunctional β2/α4 interface (Fig. 6).

Wild type nAChRs were tested before and after MTSET treatment to demonstrate that there was no block in response and to provide a comparison with the mutant nAChRs (Fig. 8*A*). Incubation of oocytes with MTSET for 5 min reduced activation by ACh for $(\alpha4^{T126C}\beta2)_2\beta3$ nAChRs by ~25–30% of the original ACh response ($p = 0.0061$) (Fig. 8, *B* and *C*). However, there was no block of response to a saturating (100 nM) concentration of sazetidine-A in this mutant (Fig. 8*B*). This confirms the idea that sazetidine-A can bind to and activate the α4/β2 sites but not β3/α4 sites.

In addition to the β3/α4 interface, we also investigated whether the β2/β3 interface formed a functional ACh binding site by mutating threonine 123 at the minus face of β3 to a cysteine. Unlike the β3/α4 interface, the β2/β3 interface did not form an ACh binding site. When $\beta3^{T123C}$ was co-expressed with the β2-α4 dimeric concatamer, the response after alkylation was similar to the wild type subtype (Fig. 8*D*).

This suggests that $(\alpha4\beta2)_2\beta3$ nAChRs contain three functional ACh binding sites: two within the dimeric concatamers at the two α4/β2 interfaces and one at the β3/α4 interface. The potencies and efficacies of ACh before and after MTSET alkylation for β3 containing nAChRs are presented in Table 4.

MTSET Blocks Activation from the α4/α5 Site—We next investigated whether an ACh binding site existed at the α4/α5 interface that formed when co-expressing a constrained α4-β2 dimeric concatamer with α5. To characterize any block of ACh activation from the α4/α5 site, the $\alpha5^{C2S,\ T139C}$ subunit was co-expressed with α4-β2 dimeric concatamer (Fig. 9*A*). The cysteine-null $\alpha5^{C2S}$ subunit was used as the negative control (Fig. 9*A*).

MTSET blocks activation from the α4/α5 site, reducing the response to 45.80 ± 0.05% after alkylation (Fig. 9*B*). These nAChRs are thought to have one conventional agonist site at

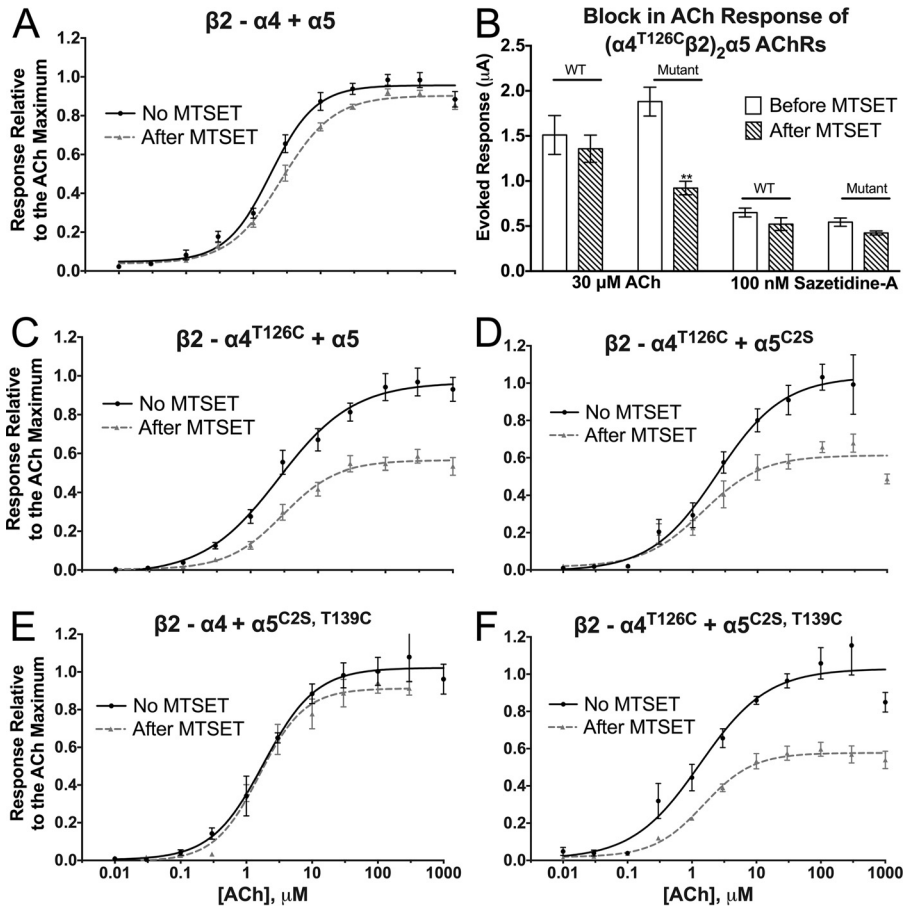

FIGURE 7. **Effect of MTSET alkylation on activation of $(\alpha4\beta2)_2\alpha5$ nAChRs.** *A*, concentration/response curves for wild type $(\alpha4\beta2)_2\alpha5$ nAChRs before and after alkylation with no significant block in response. *B*, MTSET blocked activation by ACh (30 μM), but not activation by sazetidine-A (100 nM) of mutant $(\alpha4^{T126C}\beta2)_2\alpha5$ nAChRs. MTSET had no effect on the negative control, wild type $(\alpha4\beta2)_2\alpha5$ nAChRs. A Student *t* test was used to compare responses before and after treatment of MTSET (0.5 mM). **, $p < 0.01$. *C–F*, ACh concentration/response curves before and after alkylation of mutant $(\alpha4\beta2)_2\alpha5$ nAChRs. MTSET blocked responses of $(\alpha4^{T126C}\beta2)_2\alpha5$, $(\alpha4^{T126C}\beta2)_2\alpha5^{C2S}$, and $(\alpha4^{T126C}\beta2)_2\alpha5^{C2S,\ T139C}$ nAChRs but not of $(\alpha4\beta2)_2\alpha5^{C2S,\ T139C}$ nAChRs. There is no significant difference in the block of response when compared with dimeric concatamer plus wild type α5 and the $\alpha5^{C2S}$.

TABLE 3

Summary of potencies and efficacies of ACh activating wild type and mutant $(\alpha4\beta2)_2\alpha5$ nAChRs before and after MTSET treatment

The nAChRs are expressed from concatamer β2-α4 and free α5 subunit in *Xenopus* oocytes. Efficacy indicates the maximum efficacy relative to ACh before MTSET treatment. *n* indicates the number of oocytes tested.

	β2-α4 + α5	$\beta2\text{-}\alpha4^{T126C}$ + α5	$\beta2\text{-}\alpha4^{T126C}$ + $\alpha5^{C2S}$	β2-α4 + $\alpha5^{C2S,T139C}$	$\beta2\text{-}\alpha4^{T126C}$ + $\alpha5^{C2S,T139C}$
No MTSET					
EC_{50} (μM)	1.85 ± 0.23	2.77 ± 0.38	2.22 ± 0.30	1.81 ± 0.16	1.31 ± 0.42
Efficacy (%)	99.0 ± 2.1	96.0 ± 2.4	100.4 ± 2.5	102.2 ± 1.8	103.0 ± 5.8
n_{Hill}	0.918 ± 0.074	0.824 ± 0.076	0.911 ± 0.094	1.08 ± 0.16	0.821 ± 0.186
n	7	7	3	4	4
After MTSET					
EC_{50} (μM)	2.36 ± 0.22	2.97 ± 0.33	1.33 ± 0.46	1.60 ± 0.18	1.33 ± 0.31
Efficacy (%)	92.9 ± 1.2	56.6 ± 1.3	61.4 ± 2.3	91.2 ± 2.3	58.5 ± 1.7
n_{Hill}	0.893 ± 0.039	1.05 ± 0.10	0.898 ± 0.238	1.28 ± 0.16	1.11 ± 0.13
n	7	7	3	6	10

the α4/β2 interface and one unorthodox site at the α4/α5 interface that can be blocked by MTSET. Therefore any decrease in response seen after MTSET treatment of $(\beta2\alpha4)_2\alpha5$ nAChRs can be attributed to specific block of the α4/α5 interface. MTSET only blocked ~54% of maximal response of $(\beta2\alpha4)_2\alpha5$ nAChRs. This remaining response could result from activation from the single conventional ACh site in the α4/β2 interface or inefficient blockage of the α4/α5 site.

To study whether nAChRs can be activated by a single-site, the $\beta2^{L121C}$-α4-β2-α4 tetrameric concatamer was co-expressed with β2. Free β2 assembles efficiently with β2-α4-β2-α4 tetrameric concatamer to form monopentamers, ensuring the block seen was attributed to specific block of the α4/β2 site (9). When one of the two α4/β2 sites is alkylated, there is still 39.1 ± 5.1% activation (Fig. 9). This supports the idea that one site can activate the channel, which is consistent with previous reports (34–36).

To check efficiency of blocking ACh activation under these conditions, the corresponding amino acid in the β2 subunit of the β2-α4 dimeric concatamer, leucine 121, was mutated to

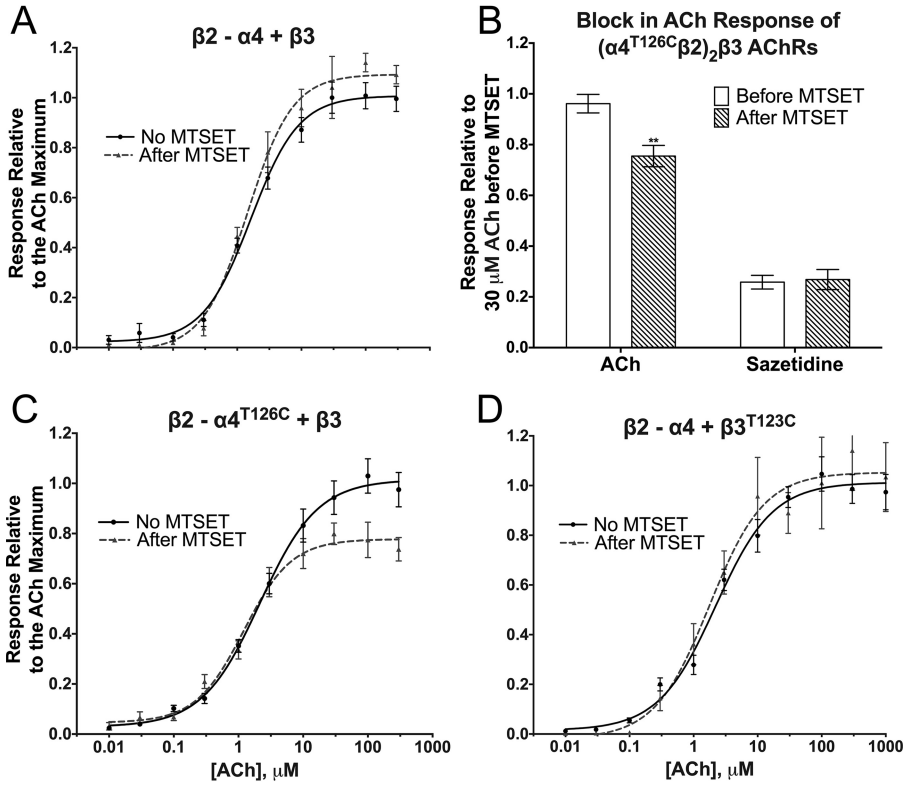

FIGURE 8. **Effect of MTSET alkylation on activation of $(\alpha4\beta2)_2\beta3$ nAChRs.** *A*, concentration/response curves of wild type $(\alpha4\beta2)_2\beta3$ nAChRs before and after 2 mM MTSET treatment. There was no significant block in response. *B*, MTSET (2 mM) blocked maximal responses of ACh (30 μM) but not sazetidine-A (100 nM) for $(\alpha4^{T126C}\beta2)_2\beta3$ nAChRs. Student *t* test was used to compare responses before and after treatment of MTSET. **, $p < 0.01$. *C* and *D*, ACh concentration/response curves before and after alkylation of mutant $(\alpha4\beta2)_2\beta3$ nAChRs. MTSET blocked responses of $(\alpha4^{T126C}\beta2)_2\beta3$ nAChRs but not of $(\alpha4\beta2)_2\beta3^{T123C}$ nAChRs.

TABLE 4

Summary of potencies and efficacies of ACh activating wild type and mutated $(\alpha4\beta2)_2\beta3$ nAChRs before and after MTSET treatment

The nAChRs are expressed from concatamer β2-α4 and free α5 subunit in *Xenopus* oocytes. Efficacy indicates the maximum efficacy relative to ACh before MTSET treatment. *n* indicates the number of oocytes tested.

	β2-α4 + β3	β2-α4^{T126C} + β3	β2-α4 + β3^{T123C}
No MTSET			
EC_{50} (μM)	1.56 ± 0.14	2.00 ± 0.20	2.11 ± 0.30
Efficacy (%)	101.2 ± 1.9	102.5 ± 2.2	101.5 ± 2.7
n_{Hill}	1.10 ± 0.09	0.890 ± 0.064	0.993 ± 0.103
n	8	9	5
After MTSET			
EC_{50} (μM)	1.48 ± 0.14	1.03 ± 0.17	1.84 ± 0.31
Efficacy (%)	109.1 ± 2.3	78.6 ± 2.5	104.9 ± 3.4
n_{Hill}	1.27 ± 0.13	0.980 ± 0.131	1.07 ± 0.16
n	5	6	5

cysteine, as previously described (9). When both of the α4/β2 sites were blocked with MTSET, blockage of response was essentially complete (Fig. 9).

This indicates that one α4/β2 was able to sufficiently activate the channel by itself if another functional binding site was deactivated, but when both of the α4/β2 sites were deactivated, the channel was not able to open with only the α4/α4 binding site. Therefore, the remaining response seen in MTSET-treated $(\beta2\alpha4)_2\alpha5$ nAChRs is likely from activation from the single conventional ACh site in the α4/β2 interface.

Presence of Pentameric α5β2 Assemblies without Functional ACh Binding Sites—Because MTSET blocks activation from α5/α4 and α4/α5 sites, α5 can assemble like a conventional α4 or β2 subunit to form an ACh binding site. We showed that the β2/α5 site did not form an ACh site (Figs. 5 and 7*E*). To investigate whether α5/β2 forms an ACh binding site, we injected oocytes with free β2 and α5. Any response detected should result from activation of α5/β2 site.

We first confirmed that α5 and β2 assembles into pentameric nAChRs using sucrose gradient sedimentation (Fig. 10*A*). These sucrose gradient fractions were immunoisolated by mAb210 (against α5 subunit) and detected by ^{125}I-mAb 295 (against β2 subunit) to study assembly of nAChRs containing both β2 and α5 subunits. β2 and α5 monomeric subunits assembled to form aggregates that sedimented at nearly the size of 9.5S *Torpedo* nAChR monomers and 13S dimers. Aggregates at the size of 13S dimers of *Torpedo* nAChRs suggest the presence of dipentamers (Fig. 10*B*). Dipentamers might form through disulfide linking of cysteines near the N terminus of α5. *Torpedo* nAChR dipentamers are linked by disulfide bonds between cysteines at the C terminus of δ subunits (37).

We next studied whether these pentameric and dipentameric α5β2 nAChRs reached the surface and responded to ACh activation. Live *Xenopus* oocytes were labeled with 1.13 ± 0.15 fmol of ^{125}I-mAb 295, ~4-fold higher than nonspecific labeling (Fig. 10*B*). Although α5β2 nAChRs expressed on the oocyte surface, no functional response was detected when various concentrations of ACh were tested. In addition, there were no high affinity epibatidine binding sites detected when the extracts were incubated with 1 nM ^{3}H-labeled epibatidine for 2 h at room temperature on mAb 295-coated Immulon wells. This

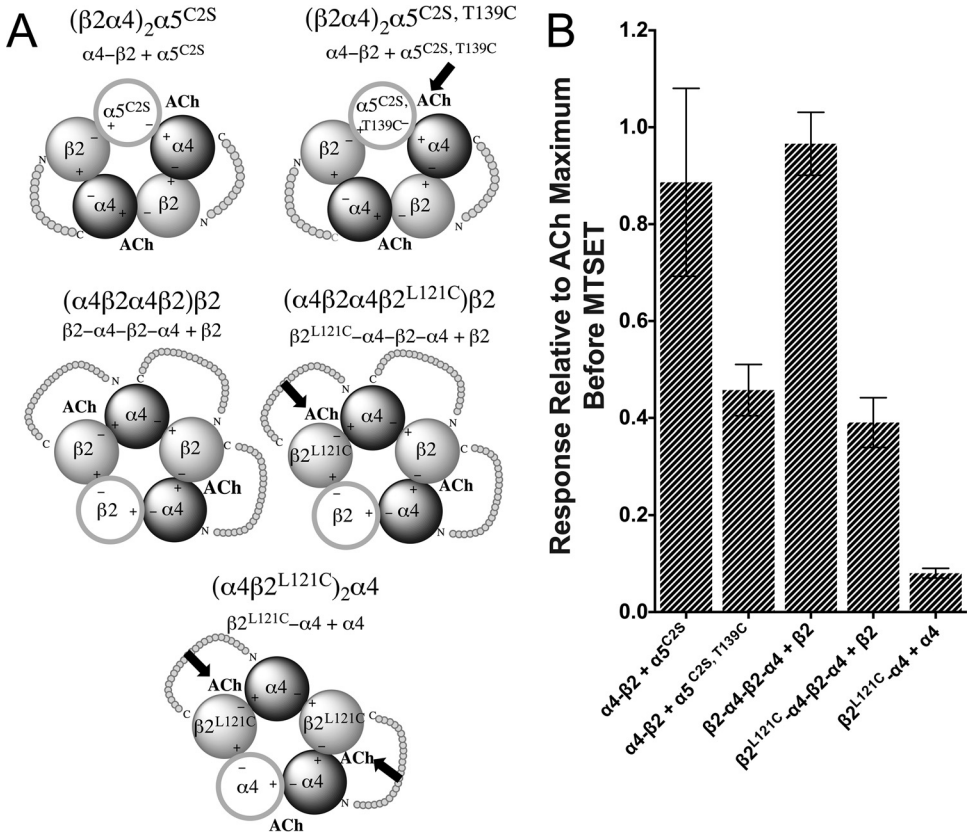

FIGURE 9. **Single-site activation of nAChRs.** *A*, schematic illustration of nAChRs expressed from concatamers and free subunit. MTSET does not react with wild type cysteine-null pseudo wild type $(\beta2\alpha4)_2\alpha5^{C2S}$ or $(\alpha4\beta2\alpha4\beta2)\beta2$ nAChRs. MTSET blocks one or two ACh sites and leaves a single ACh site in $(\alpha4^{L121C}\beta2\alpha4\beta2)\beta2$, $(\beta2\alpha4)_2\alpha5^{C2S,T139C}$, and $(\alpha4\beta2^{L121C})_2\alpha4$ nAChRs. *B*, effect of MTSET on activation of nAChRs by ACh (300 μM). Almost full response was seen for cysteine-null pseudo wild type $(\beta2\alpha4)_2\alpha5^{C2S}$ or wild type $(\alpha4\beta2\alpha4\beta2)\beta2$ nAChRs, partial response (45.6 ± 5.3 and 39.1 ± 5.1%) was seen for $(\beta2\alpha4)_2\alpha5^{C2S, T139C}$ and $(\alpha4\beta2\alpha4\beta2^{L121C})\alpha4$ nAChRs, and little response was seen after alkylation of $(\alpha4\beta2^{L121C})_2\alpha4$ nAChRs.

suggests that the $\alpha5\beta2$ oligomers most likely form both $\beta2/\alpha5$ and $\alpha5/\beta2$ interfaces, neither activated by ACh.

Discussion

Discovery of an $\alpha4/\alpha4$ interface that formed an unorthodox ACh binding site that greatly potentiated the effect of the two orthodox $\alpha4/\beta2$ ACh binding sites and is a target for the site-selective agonist drug NS9283 altered our understanding of how nAChRs work (6, 9). Here we show that $\alpha5$ and $\beta3$ subunits, which were previously not thought to form ACh binding sites, can form $\alpha5/\alpha4$, $\beta3/\alpha4$, and $\alpha4/\alpha5$ ACh binding sites. The $\alpha5/\alpha4$ ACh binding site increases the response from $(\alpha4\beta2)_2\alpha5$ nAChRs almost 2-fold. $\alpha5$ subunit greatly increases the Ca^{2+} permeability of $(\alpha4\beta2)_2\alpha5$ nAChRs (38). Increased response and high Ca^{2+} permeability caused by the presence of $\alpha5$ makes the $\alpha5/\alpha4$ ACh binding site on this nAChR subtype an appealing drug target. Unorthodox sites may be useful for targeting drugs that can be exceptionally specific for important nAChR subtypes. The unique binding sites at the $\alpha5/\alpha4$ and $\beta3/\alpha4$ interfaces are sites at which ACh site-selective agonists might act, much as NS9283 is able to act as an ACh site-selective agonist at the unique $\alpha4/\alpha4$ interfaces of $(\alpha4\beta2)_2\alpha4$ nAChRs to potentiate their function (8, 9).

It has been previously assumed that $\alpha5$ and $\beta3$ subunits cannot participate in forming ACh binding sites but do play a role in increasing Ca^{2+} permeability, sensitivity to activation, expression, and further up-regulation by nicotine for various $\alpha4\beta2^*$ nAChRs (13–15). In $(\alpha4\beta2)_2\alpha4$ nAChRs, the $\alpha4$ subunit occupies the accessory position and forms a low affinity ACh site at the $\alpha4/\alpha4$ interface. We investigated whether the $\alpha5$ and $\beta3$ subunits act similar to the $\alpha4$ subunit in $\alpha4\beta2$ nAChRs to form an ACh binding site at the $\alpha5/\alpha4$ and $\beta3/\alpha4$ interfaces of $(\alpha4\beta2)_2\alpha5$ and $(\alpha4\beta2)_2\beta3$ nAChRs.

First, we showed that the $\alpha5$ subunit can form a functional ACh binding site at the $\alpha5/\alpha4$ interface in $(\alpha4\beta2)_2\alpha5$ nAChRs where its primary (+) face contributes to forming the subunit interface and also a site at the $\alpha4/\alpha5$ interface in $(\beta2\alpha4)_2\alpha5$ nAChRs where its complementary (−) face contributes to forming the subunit interface. Second, we showed that $\alpha5$ can only form ACh binding sites with $\alpha4$ but not $\beta2$. This is surprising because $\alpha2$, $\alpha3$, $\alpha4$, and $\alpha6$ readily form ACh binding sites with $\beta2$. However, this is consistent with the idea that unorthodox ACh binding sites have novel features that make them highly specific drug targets. The $\alpha5/\alpha4$ binding site contributes almost half of the total ACh response of $(\alpha4\beta2)_2\alpha5$ nAChRs. Lastly, we showed that, similar to $\alpha5$, $\beta3$ subunits are able to form a functional ACh binding site at $\beta3/\alpha4$ interfaces in $(\alpha4\beta2)_2\beta3$ nAChRs. The accessory $\beta3$ subunit, in $(\alpha4\beta2)_2\beta3$ nAChRs, was able to form a functional ACh binding site at the $\beta3/\alpha4$ interface, contributing ~30% of the ACh response.

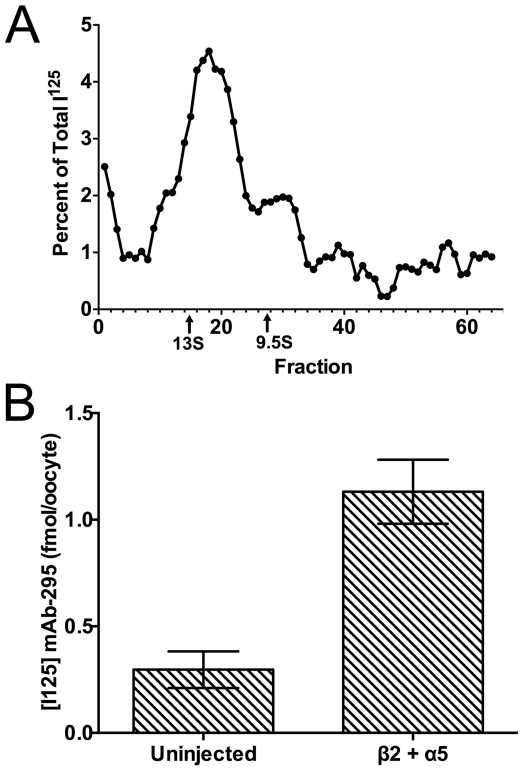

FIGURE 10. **Sucrose gradient sedimentation and surface expression of oocytes injected with free $\beta 2$ + free $\alpha 5$.** *A*, sucrose gradient sedimentation of Triton X-100 extract from oocytes injected with $\beta 2$ and $\alpha 5$. Components containing $\alpha 5$ subunits of the 63 sucrose fractions were immunoisolated using mAb 210-coated wells. $\alpha 5\beta 2$ nAChRs in these wells were then quantified using I^{125}-mAb 295 (against $\beta 2$ subunit). An internal standard in the gradient was *Torpedo* nAChR that was resolved into 9.5S monomers and 13S dimers. *Arrows* indicate the locations of the monomer and dimer peaks of *Torpedo* nAChRs. The gradient revealed that the wild type $\beta 2$ and $\alpha 5$ free subunits associated to form aggregates that sedimented at nearly the size of 9.5S *Torpedo* nAChR monomers and 13S dimers of Torpedo nAChRs. *B*, surface expression of nAChRs in oocytes injected with $\beta 2$ and $\alpha 5$ subunits. Radioactively labeled ^{125}I-mAb 295 to $\beta 2$ subunit was used to determine surface expression of nAChRs, and uninjected oocytes were used to determine nonspecific binding.

A previous study concluded that a functional $\alpha 5/\alpha 4$ binding site was not present in mouse $(\alpha 4\beta 2)_2\alpha 5$ nAChRs (39). In their studies, when the aromatic box residues in $\alpha 5$ were mutated to inhibit the interaction with the quaternary amine of ACh in $\alpha 5$, they observed no change in EC_{50} and concluded that there is no ACh binding site present at the $\alpha 5/\alpha 4$ interface. However, these mutations did cause a large decrease in the amplitude of response, which is consistent with our findings that the response is potentiated by a third ACh site present at the $\alpha 5/\alpha 4$ interface.

It has previously been reported that $\alpha 4/\alpha 5$ may form a functional ACh binding site (40). Our results are consistent with this observation.

Our data suggest that neither $\alpha 5/\beta 2$ nor $\beta 2/\alpha 5$ can form ACh binding sites. It is known that $\alpha 3/\beta 2$ forms ACh binding sites but $\beta 2/\alpha 3$ does not (41). However, $\beta 2/\alpha 3$ can be activated by the cholinergic agonist morantel, allowing morantel to potentiate the ACh response of $(\alpha 3\beta 2)_2\beta 2$ AChRs (41). This suggests that with a suitable cholinergic agonist, $\beta 2/\alpha 5$ or $\alpha 5/\beta 2$ might also be activated.

In conclusion, unorthodox ACh binding sites can form at the $\alpha 5/\alpha 4$ and $\beta 3/\alpha 4$ interfaces in $(\alpha 4\beta 2)_2\alpha 5$ and $(\alpha 4\beta 2)_2\beta 3$ nAChRs and at the $\alpha 4/\alpha 5$ in $(\beta 2\alpha 4)_2\alpha 5$ nAChRs. Looking forward, these unique interfaces can be targets for unique drugs, specifically site-selective agonists to bind to them for potential treatment of diseases or nicotine addiction. These unorthodox sites provide reason to believe that unorthodox sites might also exist at $\beta 3/\alpha 6$ interfaces. This site would provide a specific target on the complex $(\alpha 6\beta 2)(\alpha 4\beta 2)\beta 3$ nAChR subtype that is important in regulating dopamine release and potentially important in smoking cessation therapy and other applications associated with learning and motor control (15, 16). The synthesis of specific drugs that can selectively bind to these unorthodox sites might play a significant role in the treatment of nicotine addiction through activation of $(\alpha 4\beta 2)_2\alpha 5$ (29) or antagonism of $(\alpha 6\beta 2)(\alpha 4\beta 2)\beta 3$ nAChRs (18).

Experimental Procedures

Chemicals—MTSET was purchased from Toronto Research Chemicals Inc. (North York, Canada). NS9283 was synthesized as described (42). 25 and 10 mM stocks of NS9283 were prepared in DMSO. MTSET solutions were freshly prepared from solid daily and kept on ice until used. Dilutions of all drugs were prepared daily in ND96 testing buffer before use. All other chemicals were purchased from Sigma-Aldrich unless otherwise noted.

Preparation of cDNAs and cRNAs, Mutagenesis—Human $\beta 2$ and $\alpha 4$ cDNAs were cloned as described (43, 44). cDNA for human $\alpha 5$ was provided by Dr. Francesco Clementi (University of Milan, Milan, Italy), and human $\beta 3$ was provided by Christopher Grantham (Janssen Research Foundation, Beerse, Belgium) (15). Syntheses of concatamers, $\beta 2$-$(AGS)_6$-$\alpha 4$ (abbreviated $\beta 2$-$\alpha 4$), $\alpha 4$-$(AGS)_6$-$\beta 2$, and $\beta 2$-$(QAP)_n$-$\alpha 4$-$(QAP)_n$-$\beta 2$ (abbreviated $\beta 2$-$\alpha 4$-$\beta 2$) (abbreviated $\alpha 4$-$\beta 2$) were described (30, 45).

Point mutations to various subunits were introduced using the PfuUltra high fidelity DNA polymerase (Agilent, Santa Clara, CA) or the QuikChange site-directed mutagenesis kit (Stratagene, La Jolla CA), following the manufacturer's instructions. Two separate point mutations were introduced in $\alpha 5$. A threonine to cysteine mutation at position 139 was introduced to allow alkylation of ACh site at minus face of $\alpha 5$ subunit. To prevent nonspecific modification or any potential disulfide formations between the single free cysteine at position 2 of $\alpha 5$, this cysteine was mutated to serine. One point mutation was introduced in $\beta 3$. The threonine present at position 123 in the minus side of $\beta 3$ was mutated to a cysteine. Mutated dimeric concatamers, $\beta 2^{L121C}$-$(AGS)_6$-$\alpha 4$ (abbreviated $\beta 2^{L121C}$-$\alpha 4$) and $\beta 2$-$(AGS)_6$-$\alpha 4^{T126C}$ (abbreviated $\beta 2$-$\alpha 4^{T126C}$), were prepared as described (9). All oligonucleotides and the amino acids mutated are listed in Table 2. The mature amino acid sequences were used to number nAChR subunits.

To prepare the $\beta 2^{L121C}$-$\alpha 4$-$\beta 2$-$\alpha 4$ tetrameric concatamer, the $\beta 2^{L121C}$-$\alpha 4$ dimeric concatamer and the $\beta 2$-$\alpha 4$-$\beta 2$ trimeric concatamer were cut by BsiWI restriction enzyme unique to $\beta 2$ subunit. The 3390-bp BsiWI fragment from $\beta 2$-$\alpha 4$-$\beta 2$ trimeric concatamer was inserted into $\beta 2^{L121C}$-$\alpha 4$ concatamer using T4 DNA ligase (New England Biolabs). The correct clone was cho-

sen from the one that contained two fragments, 3400 and 7100 bp, after digestion by BstEII restriction enzyme (unique for α4).

All mutagenesis and ligation products were transformed into XL-10 Gold Ultracompetent cells (Stratagene) using the protocol provided with the kit. After performing a miniprep using the FastPlasmid mini kit (5Prime, Hilden, Germany), the right clone was chosen through sequencing of the miniprep DNA. High quality DNA was purified using Qiagen plasmid midiprep kit (Qiagen). The cDNAs were linearized using restriction enzymes (AseI for β2-α4, α4, α4-β2, and β2-α4-β2-α4; PvuII for β2; and EcoRI for α5 and β3). Linearized cDNA was used as a template to prepare cRNAs using mMessage mMachine kits (Ambion, Austin, TX). SP6 RNA polymerase was used for transcribing cDNAs of α4, α5, β2, β3, β2-α4, and β2-α4-β2-α4 in pSP64 vectors. The concentrations of synthesized cDNAs and cRNAs were measured by a spectrophotometer, and their quality was determined by agarose gel electrophoresis.

Xenopus Oocyte Preparation—Oocytes were harvested from *Xenopus laevis* frogs in accordance to the approved institutional animal care and use committee protocol as described (9, 46). The oocytes were washed three times with OR2 (85.5 mM NaCl, 2 mM KCl, 1 mM $MgCL_2$, and 5 mM HEPES, pH 7.5) solution and three times with 50% Leibovitz-15 (L-15) medium (Invitrogen), 10 mM HEPES, pH 7.5, 10 units/ml penicillin, 10 μg/ml streptomycin. The oocytes were then placed in Leibovitz-15 medium for a couple hours to allow for recovery before injection.

cRNA Microinjection—Subunit cRNAs were mixed in different ratios to produce the desired constructs. Proper ratios were determined by performing expression tests with ACh only and ACh coappplied with 10 μM NS9283. If potentiation was seen with NS9283, this indicated the presence of dipentamers and the ratio was adjusted until no potentiation was seen. To obtain $(\alpha4\beta2)_2\alpha5$ nAChRs, oocytes were injected with a total of 5–10 ng of cRNA, two parts of β2-α4 to one part of free α5. To obtain $(\alpha4\beta2)_2\beta3$ nAChRs, the oocytes were injected with a total of 90 ng of cRNA, one part of β2-α4 to two parts of free β3. To obtain $(\beta2\alpha4)_2\alpha5$ nAChRs, the oocytes were injected with 150 ng of cRNA, six parts of α4-β2 to one part of free α5. To obtain (α4β2α4β2)β2 nAChRs, the oocytes were injected with 30 ng of cRNA, two parts of β2-α4-β2-α4 and one part of β2. For surface labeling assays, 60 ng of free β2 and free α5 was injected at a one to one ratio. These cRNA ratios are indicated in terms of weight. Because cysteine mutations in this study did not change protein expression, the cRNA ratios of mutants used were the same as wild type. After microinjection, the oocytes were incubated in medium made up of L-15 with 50 μg/ml gentamycin and switched out to L-15 without gentamycin before electrophysiological recording. Function was assayed 3–7 days after injection.

Surface Labeling—Radioactively labeled ^{125}I-mAb 295 to β2 was used to determine surface expression of the nAChRs (47). Surface labeling was performed on the same day as electrophysiological recording. Each set of oocytes, injected with different constructs, was placed in separate Eppendorf tubes with a total volume of 500 μl of L-15 medium containing 3% bovine serum albumin with 5 nM ^{125}I-mAb 295 at room temperature for a minimum of 3 h (47). The oocytes were washed three times to remove unbound ^{125}I-mAb 295 to β2 or until there was no change in activity measured by a Geiger counter. The oocytes were put into individual tubes, and bound ^{125}I was measured using a γ-counter. Uninjected oocytes were used as the control for nonspecific binding.

Sucrose Gradient Sedimentation—A group of 60 oocytes was homogenized in 1 ml of buffer A (50 mM Na_2HPO_4, pH 7.5, 50 mM NaCl, 5 mM EDTA, 5 mM EGTA, 5 mM benzamidine, 15 mM iodoacetamide, and 2 mM phenylmethylsulfonyl fluoride) and then pelleted by centrifuging at 13,400 rpm for 15 min at 4 °C. The pellets were resuspended by pipetting, and membrane proteins were solubilized in 150 μl of buffer A containing 2% Triton X-100 for 1 h at room temperature on a rotator. Debris was removed by centrifugation at 13,400 rpm for 15 min at 4 °C. Aliquots (150 μl) of the lysates, mixed with 1 μl of 2 mg/ml purified *Torpedo californica* electric organ nAChR, were loaded onto 11.4 ml sucrose gradients (linear 5–20% sucrose (w/w) in 10 mM sodium phosphate buffer, pH 7.5, that contained 100 mM NaCl, 1 mM NaN_3, 5 mM EDTA, 5 mM EGTA, and 0.5% Triton X-100). Gradients were centrifuged for 16 h at 40,000 rpm in a SW-41 rotor (Beckman Coulter, Fullerton, CA) at 4 °C. Fractions were collected at 15 drops/well from the bottom of the tubes and used for additional analysis. Then 50 μl of each fraction were transferred to mAb 210-coated wells to isolate α5-containing nAChRs and incubated with 5 nM ^{125}I-mAb 295 to detect β2-containing nAChRs. Another 20 μl of each fraction were transferred to mAb 210-coated wells incubated with 1 nM ^{125}I-α-bungarotoxin overnight at 4 °C to isolate and detect α1-containing *T. californica* nAChRs, which are used as molecular mass standards. Afterward, the wells were washed three times with PBS and 0.5% Triton X-100, and bound ^{125}I-mAb 295 and ^{125}I-α-bungarotoxin were determined by γ-counting.

Solid Phase Radioimmunoassay—Total epibatidine binding was determined using an increasing amount of extract loaded with 1 nM [^{3}H]epibatidine (PerkinElmer Life Sciences) in a total volume of 100 μl in PBS buffer containing 0.5% Triton X-100 and 10 mM NaN_3 (47). Binding took place on a horizontal rotator for a minimum of 2 h at room temperature or overnight at 4 °C. After incubation, the wells were washed three times with 0.5% Triton X-100 in PBS before elution with 30 μl of 0.1 M NaOH solution. Bound radioactivity was determined using a 1450 Trilux Microbeta liquid scintillation counter (PerkinElmer Life Sciences) with OptiPhase scintillation fluid as described (47). Nonspecific binding was determined using uninjected oocytes.

Electrophysiology—Functions of nAChRs were measured by two-electrode voltage clamp using either a manual two-microelectrode voltage clamp amplifier setup (oocyte clamp OC-725; Warner Instrument, Hamden, CT) or OpusXpress 6000A (Molecular Devices, Union City, CA), an integrated system that provides automated impalement, voltage clamp, and simultaneous drug delivery to eight oocytes in parallel (48) (49). Voltage was held at −50 mV.

In the agonist concentration/response experiments, the oocytes first received two control applications of 300 μM ACh followed by applications of increasing concentrations of agonists. The peak amplitudes were normalized to the average of the maximum ACh response evoked by initial two controls.

Alkylation experiments were performed with the sulfhydryl agent, MTSET. The oocytes were placed in eight separate chambers and received 0.5 mM MTSET, for α5 containing nAChRs, or 2 mM MTSET, for β3 containing nAChRs, for 60 s at a rate of 0.9 ml/min, and then incubated in the MTSET for 5 min with no flow of ND96 buffer to retain the reagent in the bath. MTSET concentration was determined by finding the highest concentration that did not block the wild type nAChRs. After incubation, flow continued, and oocytes were washed for 287 s. Immediately after the washing steps, increasing concentrations of ACh were applied. The oocytes were discarded after MTSET treatment because of chemical modification. In the MTSET experiments, the peak amplitudes were normalized to the maximum ACh response prior to MTSET treatment.

In NS9283 experiments, 10 μM NS9283 was co-applied with 3 μM ACh and normalized to two controls of the same ACh concentration in which 0.1% DMSO was used as the vehicle control, instead of the 10 μM NS9283. The mean and standard error were both calculated from normalized responses in all experiments. All concentration/response values were expressed ± standard error.

The Hill equation was fit to the concentration/response relationship using a nonlinear least squares curve fit method (Kaleidagraph; Abelbeck/Synergy, Reading, PA): $I(x) = I_{max}[x^{nH}/(x^{nH} + EC_{50}{}^{nH})]$, where $I(x)$ is the peak current measured at the agonist concentration x, I_{max} is the maximum current peak at the saturating concentration, EC_{50} is the agonist concentration required to achieve half of the maximum response, and n_H is the Hill coefficient. All statistical analyses were performed using a Student's t test (two-tailed; *, $p < 0.05$; **, $p < 0.01$; and ***, $p < 0.001$).

Western Blots—Proteins from oocytes expressing linked subunits were solubilized in 2% Triton X-100, resolved into subunits by SDS-PAGE, and then transferred to Immun-Blot polyvinylidene difluoride membrane (0.2 μm; Bio-Rad). The blots were probed with rat antiserum to α4 (diluted 1:1000) or β2 (diluted 1:500) followed by ^{125}I-labeled goat anti-rat IgG (2 nM). After washing, blots were visualized by autoradiography.

Author Contributions—A. J., A. K., and J. L. designed the experiments. A. J., J. L., and J. W. wrote the manuscript. A. J. performed electrophysiological, epibatidine, and sucrose gradient sedimentation assays and analyzed data. A. J. and J. W. prepared mutant cDNAs. AK prepared concatamers and performed western blots. J. W. provided preliminary data. T. M. K. provided NS9283. All authors revised and approved the final version of the manuscript.

Acknowledgment—We thank Jie Luo for thoughtful comments on the manuscript.

References

1. Zoli, M., Pistillo, F., and Gotti, C. (2015) Diversity of native nicotinic receptor subtypes in mammalian brain. *Neuropharmacology* **96,** 302–311
2. Raftery, M. A., Hunkapiller, M. W., Strader, C. D., and Hood, L. E. (1980) Acetylcholine receptor: complex of homologous subunits. *Science* **208,** 1454–1456
3. Gotti, C., Moretti, M., Gaimarri, A., Zanardi, A., Clementi, F., and Zoli, M. (2007) Heterogeneity and complexity of native brain nicotinic receptors. *Biochem. Pharmacol.* **74,** 1102–1111
4. Albuquerque, E. X., Pereira, E. F., Alkondon, M., and Rogers, S. W. (2009) Mammalian nicotinic acetylcholine receptors: from structure to function. *Physiol. Rev.* **89,** 73–120
5. Cooper, E., Couturier, S., and Ballivet, M. (1991) Pentameric structure and subunit stoichiometry of a neuronal acetylcholine receptor. *Nature* **350,** 235–238
6. Mazzaferro, S., Benallegue, N., Carbone, A., Gasparri, F., Vijayan, R., Biggin, P. C., Moroni, M., and Bermudez, I. (2011) Additional acetylcholine (ACh) binding site at α4/α4 interface of $(\alpha4\beta2)_2\alpha4$ nicotinic receptor influences agonist sensitivity. *J. Biol. Chem.* **286,** 31043–31054
7. Harpsøe, K., Ahring, P. K., Christensen, J. K., Jensen, M. L., Peters, D., and Balle, T. (2011) Unraveling the high- and low-sensitivity agonist responses of nicotinic acetylcholine receptors. *J. Neurosci.* **31,** 10759–10766
8. Timmermann, D. B., Sandager-Nielsen, K., Dyhring, T., Smith, M., Jacobsen, A. M., Nielsen, E. Ø., Grunnet, M., Christensen, J. K., Peters, D., Kohlhaas, K., Olsen, G. M., and Ahring, P. K. (2012) Augmentation of cognitive function by NS9283, a stoichiometry-dependent positive allosteric modulator of α2- and α4-containing nicotinic acetylcholine receptors. *Br. J. Pharmacol.* **167,** 164–182
9. Wang, J., Kuryatov, A., Sriram, A., Jin, Z., Kamenecka, T. M., Kenny, P. J., and Lindstrom, J. (2015) An accessory agonist binding site promotes activation of $\alpha4\beta2^*$ nicotinic acetylcholine receptors. *J. Biol. Chem.* **290,** 13907–13918
10. Shahsavar, A., Ahring, P. K., Olsen, J. A., Krintel, C., Kastrup, J. S., Balle, T., and Gajhede, M. (2015) Acetylcholine-binding protein engineered to mimic the α4-α4 binding pocket in $\alpha4\beta2$ nicotinic acetylcholine receptors reveals interface specific interactions important for binding and activity. *Mol. Pharmacol.* **88,** 697–707
11. Zwart, R., Carbone, A. L., Moroni, M., Bermudez, I., Mogg, A. J., Folly, E. A., Broad, L. M., Williams, A. C., Zhang, D., Ding, C., Heinz, B. A., and Sher, E. (2008) Sazetidine-A is a potent and selective agonist at native and recombinant $\alpha4\beta2$ nicotinic acetylcholine receptors. *Mol. Pharmacol.* **73,** 1838–1843
12. Eaton, J. B., Lucero, L. M., Stratton, H., Chang, Y., Cooper, J. F., Lindstrom, J. M., Lukas, R. J., and Whiteaker, P. (2014) The unique $\alpha4(+)/(-)\alpha4$ agonist binding site in $(\alpha4)_3(\beta2)_2$ subtype nicotinic acetylcholine receptors permits differential agonist desensitization pharmacology versus the $(\alpha4)_3(\beta2)_2$ subtype. *J. Pharmacol. Exp. Ther.* **348,** 46–58
13. Gerzanich, V., Wang, F., Kuryatov, A., and Lindstrom, J. (1998) α5 subunit alters desensitization, pharmacology, Ca^{++} permeability and Ca^{++} modulation of human neuronal α3 nicotinic receptors. *J. Pharmacol. Exp. Ther.* **286,** 311–320
14. Groot-Kormelink, P. J., Boorman, J. P., and Sivilotti, L. G. (2001) Formation of functional $\alpha3\beta4\alpha5$ human neuronal nicotinic receptors in *Xenopus* oocytes: a reporter mutation approach. *Br. J. Pharmacol.* **134,** 789–796
15. Kuryatov, A., Onksen, J., and Lindstrom, J. (2008) Roles of accessory subunits in $\alpha4\beta2^*$ nicotinic receptors. *Mol. Pharmacol.* **74,** 132–143
16. Brown, R. W., Collins, A. C., Lindstrom, J. M., and Whiteaker, P. (2007) Nicotinic α5 subunit deletion locally reduces high-affinity agonist activation without altering nicotinic receptor numbers. *J. Neurochem.* **103,** 204–215
17. Mao, D., Perry, D. C., Yasuda, R. P., Wolfe, B. B., and Kellar, K. J. (2008) The $\alpha4\beta2\alpha5$ nicotinic cholinergic receptor in rat brain is resistant to up-regulation by nicotine *in vivo*. *J. Neurochem.* **104,** 446–456
18. Crooks, P. A., Bardo, M. T., and Dwoskin, L. P. (2014) Nicotinic receptor antagonists as treatments for nicotine abuse. *Adv. Pharmacol.* **69,** 513–551
19. Wang, J., Kuryatov, A., and Lindstrom, J. (2015) Expression of cloned $\alpha6^*$ nicotinic acetylcholine receptors. *Neuropharmacology* **96,** 194–204
20. Gotti, C., Guiducci, S., Tedesco, V., Corbioli, S., Zanetti, L., Moretti, M., Zanardi, A., Rimondini, R., Mugnaini, M., Clementi, F., Chiamulera, C., and Zoli, M. (2010) Nicotinic acetylcholine receptors in the mesolimbic pathway: primary role of ventral tegmental area $\alpha6\beta2^*$ receptors in mediating systemic nicotine effects on dopamine release, locomotion, and reinforcement. *J. Neurosci.* **30,** 5311–5325
21. Kuryatov, A., Berrettini, W., and Lindstrom, J. (2011) Acetylcholine receptor (AChR) α5 subunit variant associated with risk for nicotine depen-

dence and lung cancer reduces $(\alpha4\beta2)_2\alpha5$ AChR function. *Mol. Pharmacol.* **79,** 119–125
22. Fowler, C. D., and Kenny, P. J. (2014) Nicotine aversion: Neurobiological mechanisms and relevance to tobacco dependence vulnerability. *Neuropharmacology* **76,** 533–544
23. Chatterjee, S., Santos, N., Holgate, J., Haass-Koffler, C. L., Hopf, F. W., Kharazia, V., Lester, H., Bonci, A., and Bartlett, S. E. (2013) The α5 subunit regulates the expression and function of α4*-containing neuronal nicotinic acetylcholine receptors in the ventral-tegmental area. *PLoS One* **8,** e68300
24. Bailey, C. D., De Biasi, M., Fletcher, P. J., and Lambe, E. K. (2010) The nicotinic acetylcholine receptor α5 subunit plays a key role in attention circuitry and accuracy. *J. Neurosci.* **30,** 9241–9252
25. Gangitano, D., Salas, R., Teng, Y., Perez, E., and De Biasi, M. (2009) Progesterone modulation of α5 nAChR subunits influences anxiety-related behavior during estrus cycle. *Genes Brain Behav.* **8,** 398–406
26. Hoft, N. R., Corley, R. P., McQueen, M. B., Schlaepfer, I. R., Huizinga, D., and Ehringer, M. A. (2009) Genetic association of the CHRNA6 and CHRNB3 genes with tobacco dependence in a nationally representative sample. *Neuropsychopharmacology.* **34,** 698–706
27. Brunzell, D. H., Stafford, A. M., and Dixon, C. I. (2015) Nicotinic receptor contributions to smoking: insights from human studies and animal models. *Curr. Addict. Rep.* **2,** 33–46
28. Picciotto, M. R., and Kenny, P. J. (2013) Molecular mechanisms underlying behaviors related to nicotine addiction. *Cold Spring Harb. Perspect. Med.* **3,** a012112
29. Fowler, C. D., Lu, Q., Johnson, P. M., Marks, M. J., and Kenny, P. J. (2011) Habenular α5 nicotinic receptor subunit signaling controls nicotine intake. *Nature* **471,** 597–601
30. Zhou, Y., Nelson, M. E., Kuryatov, A., Choi, C., Cooper, J., and Lindstrom, J. (2003) Human $\alpha4\beta2$ acetylcholine receptors formed from linked subunits. *J. Neurosci.* **23,** 9004–9015
31. Ahring, P. K., Olsen, J. A., Nielsen, E. Ø., Peters, D., Pedersen, M. H., Rohde, L. A., Kastrup, J. S., Shahsavar, A., Indurthi, D. C., Chebib, M., Gajhede, M., and Balle, T. (2015) Engineered $\alpha4\beta2$ nicotinic acetylcholine receptors as models for measuring agonist binding and effect at the orthosteric low-affinity α4-α4 interface. *Neuropharmacology* **92,** 135–145
32. Nelson, M. E., Kuryatov, A., Choi, C. H., Zhou, Y., and Lindstrom, J. (2003) Alternate stoichiometries of $\alpha4\beta2$ nicotinic acetylcholine receptors. *Mol. Pharmacol.* **63,** 332–341
33. Papke, R. L., Stokes, C., Williams, D. K., Wang, J., and Horenstein, N. A. (2011) Cysteine accessibility analysis of the human α7 nicotinic acetylcholine receptor ligand-binding domain identifies L119 as a gatekeeper. *Neuropharmacology* **60,** 159–171
34. Williams, D. K., Stokes, C., Horenstein, N. A., and Papke, R. L. (2011) The effective opening of nicotinic acetylcholine receptors with single agonist binding sites. *J. Gen. Physiol.* **137,** 369–384
35. Lucero, L. M., Weltzin, M. M., Eaton, J. B., Cooper, J. F., Lindstrom, J. M., Lukas, R. J., and Whiteaker, P. (2016) Differential $\alpha4/\beta2$ agonist-binding site contributions to $\alpha4\beta2$ nicotinic acetylcholine receptor function within and between isoforms. *J. Biol. Chem.* **291,** 2444–2459
36. Andersen, N., Corradi, J., Sine, S. M., and Bouzat, C. (2013) Stoichiometry for activation of neuronal α7 nicotinic receptors. *Proc. Natl. Acad. Sci. U.S.A.* **110,** 20819–20824
37. Karlin, A. (2002) Emerging structure of the nicotinic acetylcholine receptors. *Nat. Rev. Neurosci.* **3,** 102–114
38. Tapia, L., Kuryatov, A., and Lindstrom, J. (2007) Ca2+ permeability of the $(\alpha4)_3(\beta2)_2$ stoichiometry greatly exceeds that of $(\alpha4)_2(\beta2)_3$ human acetylcholine receptors. *Mol. Pharmacol.* **71,** 769–776
39. Marotta, C. B., Dilworth, C. N., Lester, H. A., and Dougherty, D. A. (2014) Probing the non-canonical interface for agonist interaction with an α5 containing nicotinic acetylcholine receptor. *Neuropharmacology* **77,** 342–349
40. Jin, X., Bermudez, I., and Steinbach, J. H. (2014) The nicotinic α5 subunit can replace either an acetylcholine-binding or nonbinding subunit in the $\alpha4\beta2^*$ neuronal nicotinic receptor. *Mol. Pharmacol.* **85,** 11–17
41. Seo, S., Henry, J. T., Lewis, A. H., Wang, N., and Levandoski, M. M. (2009) The positive allosteric modulator morantel binds at noncanonical subunit interfaces of neuronal nicotinic acetylcholine receptors. *J. Neurosci.* **29,** 8734–8742
42. Jin, Z., Khan, P., Shin, Y., Wang, J., Lin, L., Cameron, M. D., Lindstrom, J. M., Kenny, P. J., and Kamenecka, T. M. (2014) Synthesis and activity of substituted heteroaromatics as positive allosteric modulators for $\alpha4\beta2\alpha5$ nicotinic acetylcholine receptors. *Bioorg. Med. Chem. Lett.* **24,** 674–678
43. Wang, F., Gerzanich, V., Wells, G. B., Anand, R., Peng, X., Keyser, K., and Lindstrom, J. (1996) Assembly of human neuronal nicotinic receptor α5 subunits with α3, β2, and β4 subunits. *J. Biol. Chem.* **271,** 17656–17665
44. Kuryatov, A., Gerzanich, V., Nelson, M., Olale, F., and Lindstrom, J. (1997) Mutation causing autosomal dominant nocturnal frontal lobe epilepsy alters Ca^{2+} permeability, conductance, and gating of human $\alpha4\beta2$ nicotinic acetylcholine receptors. *J. Neurosci.* **17,** 9035–9047
45. Wang, J., Kuryatov, A., Jin, Z., Norleans, J., Kamenecka, T. M., Kenny, P. J., and Lindstrom, J. (2015) A novel $\alpha2/\alpha4$ subtype-selective positive allosteric modulator of nicotinic acetylcholine receptors acting from the c-tail of an α subunit. *J. Biol. Chem.* **290,** 28834–28846
46. Gerzanich, V., Kuryatov, A., Anand, R., and Lindstrom, J. (1997) "Orphan" α6 nicotinic AChR subunit can form a functional heteromeric acetylcholine receptor. *Mol. Pharmacol.* **51,** 320–327
47. Kuryatov, A., Luo, J., Cooper, J., and Lindstrom, J. (2005) Nicotine acts as a pharmacological chaperone to upregulate human $\alpha4\beta2$ acetylcholine receptors. *Mol. Pharmacol.* **68,** 1839–1851
48. Papke, R. L., and Stokes, C. (2010) Working with OpusExpress: methods for high volume oocyte experiments. *Methods* **51,** 121–133
49. Gerzanich, V., Anand, R., and Lindstrom, J. (1994) Homomers of α8 and α7 subunits of nicotinic receptors exhibit similar channel but contrasting binding site properties. *Mol. Pharmacol.* **45,** 212–220